

# Lineage tracing of murine adult hematopoietic stem cells reveals active contribution to steady-state hematopoiesis

Richard H. Chapple,<sup>1,\*</sup> Yu-Jung Tseng,<sup>2,\*</sup> Tianyuan Hu,<sup>1</sup> Ayumi Kitano,<sup>1</sup> Makiko Takeichi,<sup>1</sup> Kevin A. Hoegenauer,<sup>1</sup> and Daisuke Nakada<sup>1,2</sup>

<sup>1</sup>Department of Molecular & Human Genetics and <sup>2</sup>Graduate Program in Translational Biology and Molecular Medicine, Baylor College of Medicine, Houston, TX

## Key Points

- HSCs contribute robustly to steady-state hematopoiesis.
- Platelets receive extensive influx from HSCs compared with other myeloid or lymphoid cells.

Characterization of hematopoietic stem cells (HSCs) has advanced largely owing to transplantation assays, in which the developmental potential of HSCs is assessed generally in nonhomeostatic conditions. These studies established that adult HSCs extensively contribute to multilineage hematopoietic regeneration upon transplantation. On the contrary, recent studies performing lineage tracing of HSCs under homeostatic conditions have shown that adult HSCs may contribute far less to steady-state hematopoiesis than would be anticipated based on transplantation assays. Here, we used 2 independent HSC-lineage-tracing models to examine the contribution of adult HSCs to steady-state hematopoiesis. We show that adult HSCs contribute robustly to steady-state hematopoiesis, exhibiting faster efflux toward the myeloid lineages compared with lymphoid lineages. Platelets were robustly labeled by HSCs, reaching the same level of labeling as HSCs by 1 year of chase. Our results support the view that adult HSCs contribute to the continuous influx of blood cells during steady-state hematopoiesis.

## Introduction

Our understanding of the cellular character and the molecular mechanisms governing hematopoietic stem cells (HSCs) has relied largely on transplantation assays. Bone marrow transplantation has proven the existence of HSCs,<sup>1-3</sup> shed light on the mechanisms that regulate self-renewal and multilineage differentiation,<sup>4-6</sup> identified multiple cell-surface markers to purify HSCs,<sup>7-9</sup> and revealed heterogeneity within the HSC pool.<sup>10-13</sup> In particular, use of sophisticated cell-surface markers and transplantation methods have documented self-renewal and multilineage differentiation of single prospectively isolated HSCs.<sup>7,8,11,13-15</sup> Although these studies have lent crucial insights into the fundamental properties of HSCs, they are limited by the fact that the potential of HSCs are assessed in a nonphysiological transplantation setting involving myeloablation. While understanding the potential of HSCs has clinical significance, improving our understanding of how HSCs behave in steady state may provide novel insights into the pathophysiology of hematological disorders involving HSCs.

Recent advances in genetic labeling of HSCs in situ have provided novel insights into the behavior of HSCs in steady state. A study using transposon-based barcoding of hematopoietic cells revealed that steady-state hematopoiesis is supported by a large number of transient clones that receive little influx from HSCs.<sup>16</sup> Another study that used an HSC-specific inducible Cre system driven by the *Tie2* promoter (*Tie2*<sup>MCM</sup>; referred to as *Tie2-CreER*) found that HSCs labeled by *Tie2-CreER* have slow contribution to hematopoiesis, such that an equilibrium between labeled HSCs and their progeny is not reached within the lifespan of mice.<sup>17</sup> The implication of this study is that, despite the fact that they exhibit limited self-renewal capacity in transplantation assays, multipotent progenitors (MPPs) are capable of extensive self-renewal in steady state and are the major contributors of hematopoiesis. The *Tie2-CreER* strain

was also used in a Cre-loxP-mediated barcoding study, which also supported the notion that HSCs have a relatively small contribution to steady-state hematopoiesis.<sup>18</sup> Consistent with these findings, ablation of >90% of HSCs had minimal impact on steady-state hematopoiesis.<sup>19</sup> By contrast, a recent lineage-tracing study using *Pdzk1ip1-CreER* strain reported extensive contribution of labeled HSCs to hematopoiesis in steady state.<sup>20</sup> Furthermore, labeling HSC clones with multiple fluorescent proteins in HUE mice revealed that native hematopoiesis is supported by several large clones that are relatively stable, although some clones fluctuated in terms of their size.<sup>21</sup> Thus, the clonal behavior of HSCs during steady-state hematopoiesis remains unclear. Additional work with different mouse models is needed to comprehensively understand the steady-state behavior of HSCs.

Here, we used 2 independent lineage-tracing models to demonstrate that HSCs actively contribute to steady-state hematopoiesis. We identified *Krt18* as a gene enriched in HSC and performed lineage tracing of HSCs using *Krt18-CreER*. We also used a recently described mouse model to lineage trace HSCs by the expression of *Fgd5*.<sup>22</sup> The genetically labeled HSCs actively contributed to hematopoiesis, with particularly rapid efflux into platelets and myeloid cells. Our results support the model in which immunophenotypically defined HSCs are active participants in hematopoietic homeostasis.

## Materials and methods

### Mice

The mouse alleles used in this study were *Krt18-CreER* (Tg(KRT18-cre/ERT2)23Blpn/J, Jackson Laboratory [JAX] stock 017948),<sup>23</sup> *Fgd5-ZsGreen-2A-CreER*,<sup>22</sup> *Rosa26-LSL-YFP* (JAX stock 006148), and *Rosa26-LSL-tdTomato* (JAX stock 007909) on a C57BL/6 background. CD45.1 mice (B6.SJL-*Ptprca*<sup>a</sup> *Pepcb*<sup>b</sup>/BoyJ, JAX stock 002014) were used as transplant recipient mice. Mice of both sexes were used. Mice were housed in Association for Assessment and Accreditation of Laboratory Animal Care-accredited, specific-pathogen-free animal care facilities at Baylor College of Medicine (BCM), and all procedures were approved by the BCM Institutional Animal Care and Use Committee.

### Tamoxifen and 5-FU treatment

Mice were injected intraperitoneally with 100  $\mu$ L corn oil containing 2.5 mg tamoxifen (Sigma, St. Louis, MO) every day for 5 days. 5-fluorouracil (5-FU) (Sigma) dissolved in phosphate-buffered saline (PBS) to a final concentration of 50 mg/mL was injected 2 weeks after the first tamoxifen treatment with a single dose of 150 mg/kg.

### Transplantation

Male 10- to 12-week-old CD45.1 mice were randomly assigned to groups after receiving 2 doses of radiation (500 cGy) administered at least three hours apart (total 1000 cGy). Thirty yellow fluorescent protein (YFP)<sup>+</sup> or YFP<sup>-</sup> HSCs were transplanted retro-orbitally, along with  $5 \times 10^5$  CD45.1 whole bone marrow cells, into each recipient.

### Flow cytometry and HSC isolation

Bone marrow cells were either flushed from the long bones (tibiae and femurs) or isolated by crushing the long bones (tibiae and femurs), pelvic bones, and vertebrae with mortar and pestle in Hank's buffered salt solution without calcium and magnesium, supplemented with 2% heat-inactivated bovine serum (Gibco, Grand Island, NY). Cells were triturated and filtered through a nylon screen

(100  $\mu$ m; Sefar America, Kansas City, MO) or a 40- $\mu$ m cell strainer (Fisher Scientific, Pittsburg, PA) to obtain a single-cell suspension. For isolation of CD150<sup>+</sup>CD48<sup>-</sup>Lineage<sup>-</sup>Sca-1<sup>+</sup>c-kit<sup>+</sup> HSCs, bone marrow cells were incubated with phycoerythrin (PE)-Cy5-conjugated anti-CD150 (TC15-12F12.2; BioLegend, San Diego, CA), PE-conjugated (HM48-1; BioLegend), or PE-Cy7-conjugated anti-CD48, allophycocyanin (APC)-conjugated anti-Sca-1 (Ly6A/E; E13-6.7), and biotin-conjugated anti-c-kit (2B8) antibody, in addition to antibodies against the following fluorescein isothiocyanate (FITC)-conjugated lineage markers: CD41 (MWRReg30; BD Biosciences, San Jose, CA), Ter119, B220 (6B2), Gr-1 (8C5), CD2 (RM2-5), CD3 (KT31.1), and CD8 (53-6.7). For the isolation of YFP<sup>+</sup> HSCs, the FITC channel was left open, and PE-conjugated lineage markers were used instead. For the isolation of tdTomato<sup>+</sup> (which are also ZsGreen<sup>+</sup>) HSCs, the FITC and PE channels were left open, and Brilliant Violet 421 (BV421)-conjugated lineage markers were used instead. For isolation of CD34<sup>+</sup>CD16/32<sup>-</sup>Lineage<sup>-</sup>Sca-1<sup>-</sup>c-kit<sup>+</sup> megakaryocyte-erythrocyte progenitors (MEPs), CD34<sup>+</sup>CD16/32<sup>-</sup>Lineage<sup>-</sup>Sca-1<sup>-</sup>c-kit<sup>+</sup> common myeloid progenitors (CMPs), and CD34<sup>+</sup>CD16/32<sup>+</sup>Lineage<sup>-</sup>Sca-1<sup>-</sup>c-kit<sup>+</sup> granulocyte-macrophage progenitors (GMPs), bone marrow cells were incubated with AF700-conjugated anti-CD34 (RAM34; eBioscience, San Diego, CA), PE-Cy7-conjugated anti-CD16/32 (93; BioLegend), PE-Cy5-conjugated anti-Sca-1 (Ly6A/E; E13-6.7), and biotin-conjugated anti-c-kit (2B8) antibody, in addition to antibodies against the following PE- or BV421-conjugated lineage markers: Ter119, B220 (6B2), Gr-1 (8C5), Mac-1 (M1/70), CD2 (RM2-5), CD3 (KT31.1), and CD8 (53-6.7). Unless otherwise noted, antibodies were obtained from BioLegend, BD Biosciences, or eBioscience (San Diego, CA). Biotin-conjugated antibodies were visualized using streptavidin-conjugated APC-Cy7. HSCs were sometimes pre-enriched by selecting c-kit<sup>+</sup> cells using paramagnetic microbeads and autoMACS (Miltenyi Biotec, Auburn, CA). Nonviable cells were excluded from sorts and analyses using the viability dye 4',6-diamidino-2-phenylindole (DAPI) (1  $\mu$ g/mL). To analyze hematopoietic lineage composition, bone marrow cells or splenocytes were incubated with PerCP-Cy5.5-conjugated anti-B220, PE- or BV421-conjugated anti-Ter119, APC-conjugated anti-CD3, APC-eFluor780-conjugated anti-Mac-1 (M1/70), and PE-Cy7-conjugated anti-Gr-1 antibodies. Platelets in the unlysed, EDTA-treated peripheral blood samples were identified as forward scatter/side scatter<sup>low</sup> CD41<sup>+</sup>Ter119<sup>-</sup> events. Flow cytometry was performed with FACSAria II, FACSCanto II, LSR II, or LSRFortessa flow cytometers (BD Biosciences).

### Quantitative real-time PCR

HSCs and other hematopoietic cells were sorted into Trizol (Life Technologies, Carlsbad, CA), and RNA was isolated according to the manufacturer's instructions. Complementary DNA was made with SuperScript VILO Master Mix (Life Technologies). Quantitative polymerase chain reaction (PCR) was performed using a ViiA7 Real-Time PCR System (Life Technologies). Each sample was normalized to  $\beta$ -actin. Data were analyzed using the  $2^{-\Delta\Delta Ct}$  method. Primers are listed in supplemental Table 1.

### Single-cell quantitative real-time PCR

A published protocol was adapted to perform single-cell quantitative PCR.<sup>24</sup> Single HSCs were sorted into 5  $\mu$ L 2 $\times$  CellsDirect reaction mix (Thermo Fisher) deposited in each well of a 96-well plate. A total of 4  $\mu$ L reaction mix (0.2  $\mu$ L SuperScript III/RT Platinum Taq mix, 2.5  $\mu$ L primer mix [final concentration of each primer, 200 nM], 1.2  $\mu$ L

RNase-free H<sub>2</sub>O, and 0.1 μL SUPERase-In) was then added to each well. Reverse transcription and preamplification was performed in a thermocycler with the following program: 50°C for 15 minutes, 70°C for 2 minutes, 95°C for 2 minutes, 18 cycles of 95°C for 15 seconds, and 60°C for 4 minutes. Samples were then treated with ExoSAP-IT (37°C for 30 minutes and 80°C for 15 minutes) to remove excess primers. Treated complementary DNA was used for real-time PCR. For visualization, ΔCt values have been scaled to a proportion of the dynamic range of expression values for each gene (minimum expression = 0.0, maximum = 1.0). Single cells that had Ct values of Actb higher than no-cell control were removed from the analysis. Primers are listed in supplemental Table 1.

## HSC immunostaining

HSCs and other populations were sorted and cytopspun on glass slides. Cells were fixed in ice-cold methanol for 5 minutes in -20°C, washed in PBS, and blocked in blocking buffer (4% goat serum, 0.4% BSA, and 0.1% NP-40 in PBS) before being incubated with anti-Krt18 antibody (PA5-14263, Thermo Fisher) diluted 1:50 in blocking buffer overnight at 4°C. Slides were rinsed and incubated with Alexa Fluor 555-conjugated goat anti-rabbit antibody (Invitrogen, Eugene, OR) at 1:500 dilution in blocking buffer containing DAPI. Images were obtained using a Leica DMI 6000B microscope.

## Quantification and statistical analysis

Data are presented as mean ± standard deviation or mean ± standard error of the mean (SEM), as indicated in the figure legends. Comparison of 2 groups was performed using an unpaired Student *t* test. Comparisons of >2 groups were performed by 1-way or 2-way analysis of variance (ANOVA). *P* < .05 was considered significant.

## Results

### *Krt18* expression is enriched in HSCs

Using the Gene Expression Commons<sup>25</sup> and the hematopoietic fingerprints<sup>26</sup> to search for genes relatively enriched in HSCs, we identified *Krt18* as a candidate gene (Figure 1A-B). *Krt18* exhibited an expression pattern similar to other reported HSC markers, such as *Pdzk1ip*,<sup>20</sup> *Fgd5*,<sup>22</sup> and *Hoxb5*<sup>27</sup> (Figure 1A-B; supplemental Figure 1A-C). *Krt18* expression was highest in HSCs, while other hematopoietic stem/progenitor cells (HSPCs) and mature cells exhibited low level of expression (Figure 1A-B). These results are consistent with a recent study that reported enriched expression of *Krt18* and *Krt7* in HSPCs, with particularly high levels in HSCs<sup>28</sup> (supplemental Figure 1D). Quantitative real-time PCR (qRT-PCR) on purified populations including CD150<sup>+</sup>CD48<sup>-</sup>lin<sup>-</sup>Sca-1<sup>+</sup>c-kit<sup>+</sup> HSCs, CD150<sup>-</sup>CD48<sup>-</sup>lin<sup>-</sup>Sca-1<sup>+</sup>c-kit<sup>+</sup> MPPs, CD150<sup>-</sup>CD48<sup>-</sup>lin<sup>-</sup>Sca-1<sup>+</sup>c-kit<sup>+</sup> hematopoietic progenitor cell 1 (HPC1), CD150<sup>+</sup>CD48<sup>+</sup>lin<sup>-</sup>Sca-1<sup>+</sup>c-kit<sup>+</sup> HPC2, and other immature and mature hematopoietic cells showed that *Krt18* is broadly expressed in HSPCs, among which HSCs exhibit particularly high expression levels (Figure 1C). Immunofluorescence staining of freshly isolated HSCs, MPPs, HPC1/2, and mature cells revealed that Krt18 protein was readily detectable in all HSCs (25 out of 25 HSCs) but was only detectable at very low levels in immature cell populations and almost undetectable in differentiated cells (Figure 1D). These results establish that high *Krt18* expression distinguishes HSCs from other hematopoietic cells.

### *Krt18-CreER* labels HSCs

*Krt18-CreER* transgenic mice have been generated and used in lineage-tracing analysis of the epidermis, exhibiting specific but relatively inefficient recombination in vibrissa Merkel cells.<sup>23</sup> We obtained *Krt18-CreER* mice and generated *Krt18-CreER*; *loxP-STOP-loxP-EYFP* mice (hereafter referred as *Krt18-CreER/YFP* mice). To initiate lineage tracing, we administered tamoxifen for 5 consecutive days and analyzed YFP expression in hematopoietic cells 2 days after the last injection (1 week; Figure 2A-B). A small fraction of bone marrow cells became YFP<sup>+</sup>, among which most were HSCs (Figure 2B; supplemental Figure 2A-B). At this time point, 2.0 ± 1.2% of HSCs were YFP<sup>+</sup>, with little to no expression of YFP in other populations, including MPPs (Figure 2C). The relatively inefficient labeling by *Krt18-CreER* appeared to be due to low expression of the *Krt18-CreER* transgene or inefficient CreER activation,<sup>23</sup> since both YFP<sup>+</sup> and YFP<sup>-</sup> HSCs expressed *Krt18* messenger RNA at similar levels, and *Krt18* was detected in most HSCs in a single-cell quantitative PCR assay (supplemental Figure 3A-B). Immunophenotypic HSCs that were labeled by *Krt18-CreER* were indeed functional HSCs, since competitive transplantation of 30 YFP<sup>+</sup> or YFP<sup>-</sup> HSCs both exhibited long-term multilineage reconstitution (Figure 2D; supplemental Figure 3C). Thus, *Krt18-CreER* allows labeling of a small fraction of HSCs in situ.

### Adult HSCs contribute to steady-state hematopoiesis

We then chased tamoxifen-injected *Krt18-CreER/YFP* mice for up to 1 year to determine the contribution of HSCs to steady-state hematopoiesis (Figure 3A-D). A small fraction of HSCs were YFP<sup>+</sup> (3.0% ± 1.7%) 1 year after the tamoxifen treatment, exhibiting a small increase in comparison with what was found immediately after tamoxifen treatment (2.0% ± 1.2%), suggesting that self-renewing HSCs were labeled by *Krt18-CreER* (Figure 3D). No background labeling was observed in a control cohort chased in parallel without tamoxifen treatment (supplemental Figure 2C). Since low levels of labeling could be observed in MPPs and HPC1/2s immediately after tamoxifen treatment (0.11% to 0.48%), it is possible that labeling of downstream cells below this threshold derives from these progenitors. However, any labeling beyond this threshold can be interpreted as being derived from a cell population with initial labeling frequency higher than the threshold, which in this case is the HSC fraction (Figure 3A). At 4 weeks after the first injection, we found YFP<sup>+</sup> cells emerging in many fractions, including the lin<sup>-</sup>Sca-1<sup>+</sup>c-kit<sup>+</sup> (LSK) fraction, myeloid progenitors (GMPs, CMPs, and MEPs), myeloid cells, and platelets (Figure 3B). To quantify the extent to which progenitors and mature cells become labeled downstream of HSCs, we normalized the YFP<sup>+</sup> frequency of each cell population to that of HSCs in the same animal (Figure 3E-H). Myeloid progenitor cells and myeloid cells were more rapidly labeled by YFP than lymphoid cells, reaching up to 60% of the level of HSC labeling by 1 year of chase (Figure 3F-H). Common lymphoid progenitors were also labeled up to 50% of the level of HSCs by 1 year of chase, paralleling the labeling of B cells in the bone marrow and peripheral blood (Figure 3F-H). In contrast, labeling of T-cells was significantly delayed compared with B-cells (Figure 3G-H). These results establish that adult HSCs contribute robustly to steady-state hematopoiesis, exhibiting faster contribution toward the myeloid lineage compared with the lymphoid lineage.

The most striking finding was the robust labeling of platelets, which exhibited rapid and substantial labeling (37 ± 11% of HSC labeling) even at 4 weeks after tamoxifen treatment (Figure 3B,H) and continued to increase over time to reach the labeling

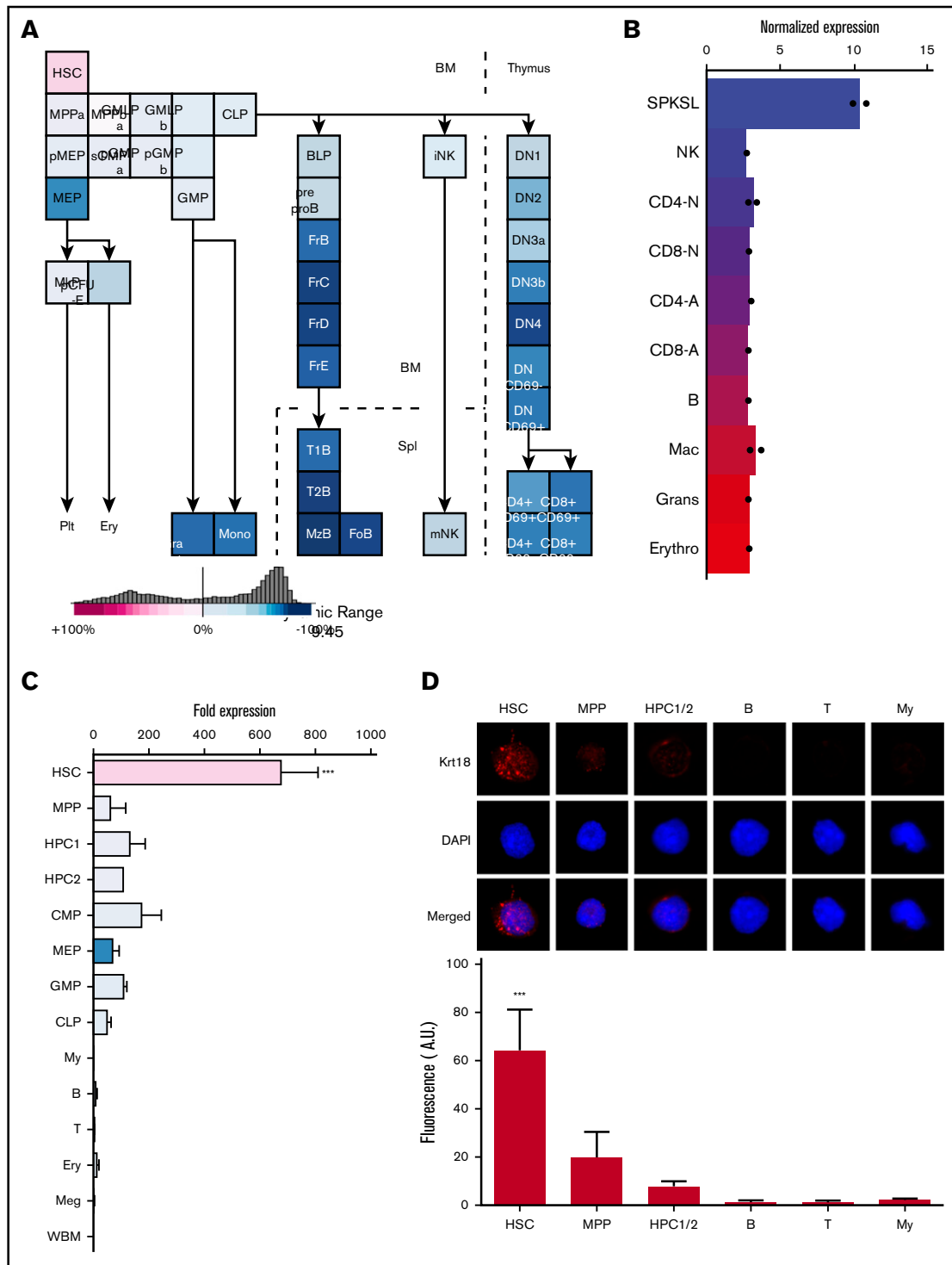


**Figure 1. HSCs exhibit high *Krt18* expression.** (A-B) Expression levels of *Krt18* in the hematopoietic system determined by the Gene Expression Commons (A; <https://gecx.riken.jp/>) and by the hematopoietic fingerprints (B; <http://franklin.imgen.bcm.tmc.edu/loligag/>). (C) Expression of *Krt18* in the hematopoietic system determined by quantitative PCR. Expression levels of *Krt18* were normalized with  $\beta$ -actin, and fold change in expression levels was normalized to the expression levels of whole bone marrow (WBM) ( $n = 3-4$ ). Color codes of each population were taken from panel A. (D) Immunofluorescence staining of HSCs and the indicated cell populations for *Krt18* protein. HSCs had significantly higher protein expression levels of *Krt18* than any other population. Signal intensities of each cell were normalized to that of a negative control (secondary antibody only). All data represent mean  $\pm$  standard deviation; \*\*\* $P < .001$  by 1-way ANOVA with post hoc Tukey's multiple comparison test against all other groups. B, B cell; BLP, earliest B-lymphoid progenitor; DN, double-negative T cell; DP, double-positive T cell; FoB, follicular B cell; FrB-D, fraction B-D B cell; GMLP, granulocyte/macrophage/lymphoid progenitor; Gra Gr+, granulocyte; MkP, megakaryocyte progenitor; mono, monocyte; My, myeloid cell; MzB, marginal zone B cell; NK, natural killer cell; p-CFU-E, pre-colony forming unit-erythrocyte; pGMP, pre-granulocyte/macrophage progenitor; pMEP, pre-megakaryocyte/erythrocyte progenitor; sCMP, strict common myeloid progenitor; T, T cell.

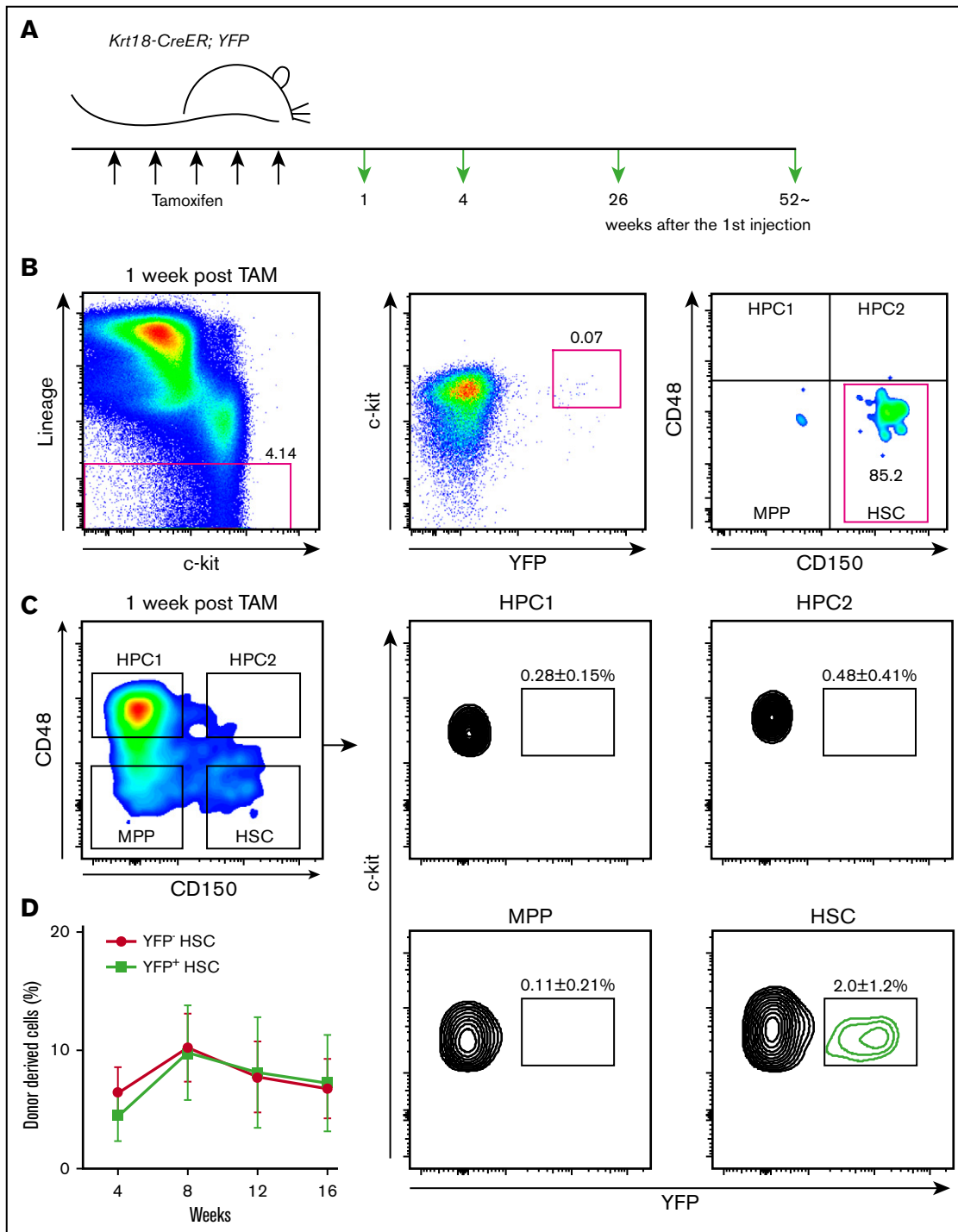


**Figure 2. *Krt18-CreER* labels HSCs.** (A) Experimental setup. *Krt18-CreER;YFP* mice (3-6 months old) were injected with tamoxifen for 5 days and analyzed at 1, 4, 26, and ~52 weeks after the first injection. (B) Representative flow cytometry plot at 1 week after the first tamoxifen treatment. A total of 80% to 90% of Lineage<sup>-</sup>YFP<sup>+</sup> cells were HSCs. The numbers indicate the frequencies of cells in the indicated gate in respect to the parental gate. (C) Representative flow cytometry plots of LSK fraction separated by CD150 and CD48 to identify HSCs, MPPs, HPC1, and HPC2 at 1 week. Approximately 2% of HSCs were YFP<sup>+</sup>, whereas YFP<sup>+</sup> cells in other immature populations were rare. (D) 30 YFP<sup>+</sup> and YFP<sup>-</sup> HSCs were isolated and competitively transplanted. There were no significant differences in the reconstitution levels between the 2 groups (n = 3). Error bars in panel D represent SEM.

efficiency of HSCs after one year ( $101 \pm 25\%$  of HSCs; Figure 3H). Within the immature LSK fraction, the rare HPC2 population, which has been shown to have megakaryocytic potential,<sup>29,30</sup> became labeled for >70% of the HSC labeling

frequency (Figure 3E). These results demonstrate that adult HSCs not only robustly contribute to steady-state hematopoiesis but also exhibit a strong tendency to contribute to the megakaryocytic/platelet lineage in situ.

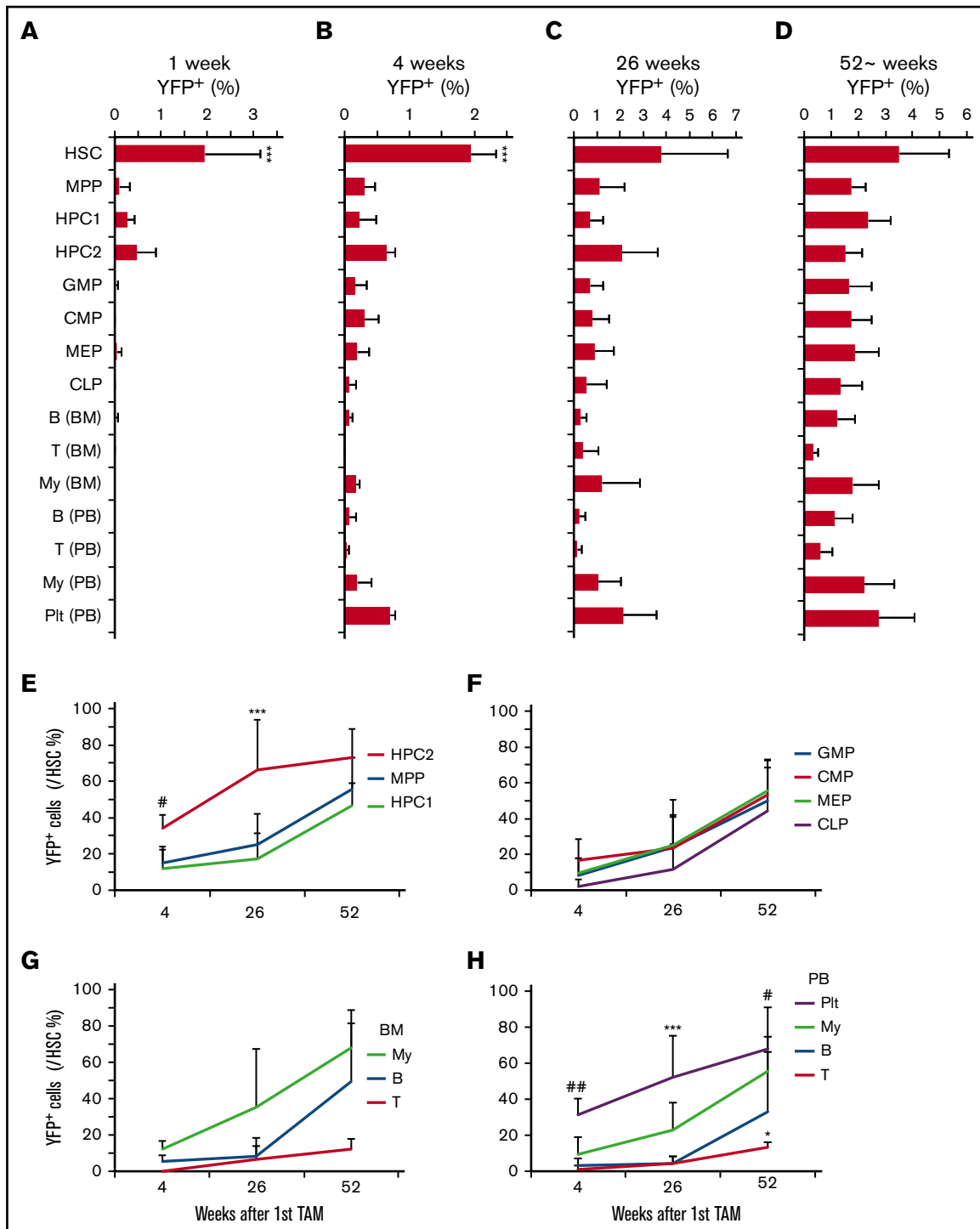


**Figure 3. HSCs labeled by *Krt18-CreER* contribute to steady-state hematopoiesis.** (A-D) Longitudinal analysis of YFP<sup>+</sup> fraction in the indicated populations at 1 (A), 4 (B), 26 (C), and ~52 (D) weeks after tamoxifen treatment (n = 4-6). (E-F) Frequencies of YFP<sup>+</sup> cells in each population relative to HSCs. (E) Frequencies of YFP<sup>+</sup> cells within the LSK fraction relative to HSCs. (F) Relative frequencies of YFP<sup>+</sup> myeloid and lymphoid progenitor cells relative to HSCs. Relative YFP<sup>+</sup> frequencies of mature myeloid cells (My), B-cells (B), and T cells (T) to HSCs in the bone marrow (BM) (G) and peripheral blood (H). All data represent mean ± standard deviation. In panels A-D, \**P* < .05, \*\**P* < .01, and \*\*\**P* < .001 (1-way ANOVA with post hoc Tukey's multiple comparison test against all other groups). In panels E-H, \**P* < .05, \*\**P* < .01, and \*\*\**P* < .001 (2-way ANOVA with post hoc Tukey's multiple comparison test against all other groups). #*P* < .05, ##*P* < .01 (post hoc Tukey's multiple comparison test between HSCs and MPP/HPC1) in panel E and between platelets (Plt) and B/T cells in panel H.

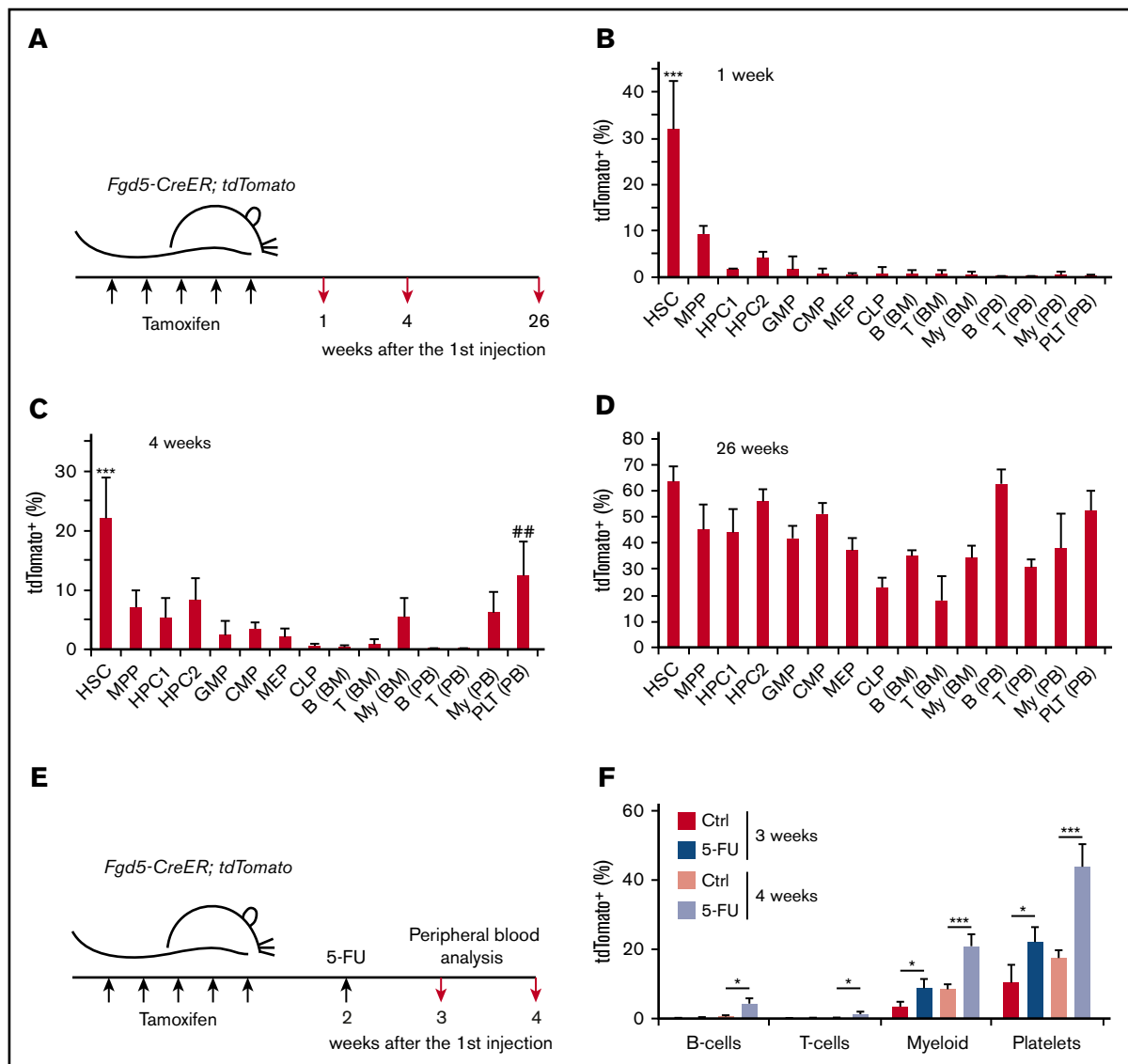


**Figure 4. HSCs labeled by *Fgd5-CreER* contribute to steady-state hematopoiesis.** (A) Experimental setup. *Fgd5-CreER; tdTomato* mice (3-6 months old) were injected with tamoxifen for 5 days and analyzed at 1, 4, and 26 weeks after the first injection. (B-D) Longitudinal analysis of *tdTomato*<sup>+</sup> fraction in the indicated populations at 1 (B), 4 (C), and 26 (D) weeks after tamoxifen treatment (n = 3-9). (E) Experimental setup to examine the effect of 5-FU treatment on *Fgd5-CreER*-based labeling. *Fgd5-CreER; tdTomato* mice were injected with tamoxifen for 5 days, then with 5-FU at 2 weeks after the first tamoxifen injection. Peripheral blood (PB) was analyzed at weeks 3 and 4 (n = 3-4). (F) Peripheral blood analysis for *tdTomato*<sup>+</sup> cells in the indicated population revealed increased *tdTomato*<sup>+</sup> cells after 5-FU treatment. All data represent mean ± SEM. In panels B-D, \*\*\**P* < .001 (1-way ANOVA with post hoc Tukey's multiple comparison test against all other groups) and ##*P* < .01 (1-way ANOVA with post hoc Tukey's multiple comparison test against all other groups except for HSC and HPC2). In panel F, \**P* < .05 and \*\*\**P* < .001 (Student *t* test). PLT, platelet.

### Lineage tracing of HSCs with *Fgd5-CreER*

To examine HSC behavior in situ with an independent CreER driver, we obtained the *Fgd5-ZsGreen-2A-CreER* strain<sup>22</sup> and crossed with a *loxP-STOP-loxP-tdTomato* reporter (hereafter referred to as *Fgd5-CreER/tdTomato* mice). *Fgd5* has shown to be specifically expressed in HSCs and the *Fgd5-CreER* allele exhibits inducible CreER activity exclusively in CD150<sup>+</sup> HSCs.<sup>22</sup> Similar to the *Krt18-CreER/YFP* mice, we treated *Fgd5-CreER/tdTomato* mice with tamoxifen for 5 consecutive days and analyzed at day 7 (Figure 4A). Consistent with the previous report, we found that *tdTomato*<sup>+</sup> cells are significantly enriched in the HSC fraction

compared with other populations at this early time point after CreER activation (Figure 4B; supplemental Figure 4A-B). Thirty-two percent ± 10% of HSCs became *tdTomato*<sup>+</sup> at 1 week after tamoxifen treatment, indicating that *Fgd5-CreER* is more efficient and labels a larger fraction of HSCs than *Krt18-CreER*. Similar to our experiments in *Krt18-CreER/YFP* mice, chasing the tamoxifen-treated *Fgd5-CreER/tdTomato* mice for 4 and 26 weeks showed that HSCs labeled by *Fgd5-CreER* also contribute robustly to steady-state hematopoiesis (Figure 4C-D). At 4 weeks after tamoxifen treatment, many cell populations, including cells in the LSK fraction (MPPs, HPC1, and HPC2) and myeloid progenitors (CMPs,

GMPs, and MEPs), became labeled with tdTomato. Within mature hematopoietic cells, myeloid cells and platelets were robustly labeled at 4 weeks. In particular, labeling in platelets was significantly higher than any other population except for HSCs and HPC2 (Figure 4C). At 26 weeks, all populations analyzed exhibited significant labeling compared with the levels observed at 1 week, with HPC2 and platelets exhibiting similar labeling frequencies as HSCs (Figure 4D). Similar to the *Krt18-CreER* lineage-tracing model, no background labeling was observed in a control cohort chased in parallel without tamoxifen treatment (supplemental Figure 4C). These results confirm the results obtained with *Krt18-CreER* and demonstrate that adult HSCs contribute robustly to steady-state hematopoiesis.

To determine whether hematopoietic stress accelerates the rate in which HSCs contribute to hematopoiesis, we injected tamoxifen-treated *Fgd5-CreER/tdTomato* mice with 5-FU to induce stress and analyzed the peripheral blood at 1 and 2 weeks after 5-FU treatment (Figure 4E). We found that the frequency of tdTomato<sup>+</sup> cells in the peripheral blood increased significantly after 5-FU treatment (Figure 4F). The frequencies of tdTomato<sup>+</sup> myeloid cells and platelets were substantially increased after 5-FU treatment, consistent with the higher contribution of HSCs to these lineages. Thus, hematopoietic stress accelerates the rate in which HSCs contribute to hematopoiesis.

## Discussion

Here, we performed lineage tracing of adult HSCs using 2 independent CreER drivers, *Krt18-CreER* and *Fgd5-CreER*. We found that adult HSCs robustly contribute to steady-state hematopoiesis, with particularly fast and robust contribution to the platelet lineage, followed by myeloid cells and B cells. Upon hematopoietic stress caused by 5-FU, the rate at which HSCs contribute to hematopoiesis was significantly accelerated, consistent with previous reports.<sup>17,20</sup> Overall, our results are consistent with a recent report<sup>20</sup> and support the conventional view that hematopoiesis receives steady influx from HSCs. A potential explanation for the discrepancy between studies using different CreER lines (*Tie2-CreER*, *Pdzk1ip1-CreER*, *Krt18-CreER*, and *Fgd5-CreER*) could be that each CreER line labels a somewhat distinct subpopulation of HSCs. Of note, a recent study demonstrated that Tie2-GFP<sup>+</sup> HSCs are distinct from Tie2-GFP<sup>-</sup> HSCs in terms of their reconstitution potential and propensity to undergo symmetric self-renewal division.<sup>14</sup>

With both *Krt18-CreER* and *Fgd5-CreER* lineage-tracing experiments, we observed slightly higher labeling efficiencies in HSCs compared with MPPs, even at the latest time point analyzed. This is consistent with the finding that a rare population of HSCs that are deeply quiescent exists in adult bone marrow.<sup>31,32</sup> Thus, although most HSCs divide and contribute to hematopoiesis via MPPs and other progenitor cells, a small subset of (genetically labeled) HSCs may remain dormant without contributing to hematopoiesis.

## References

1. Till JE, McCulloch EA. A direct measurement of the radiation sensitivity of normal mouse bone marrow cells. *Radiat Res*. 1961;14(2):213-222.
2. Becker AJ, McCulloch EA, Till JE. Cytological demonstration of the clonal nature of spleen colonies derived from transplanted mouse marrow cells. *Nature*. 1963;197(4866):452-454.
3. Siminovitch L, McCulloch EA, Till JE. The distribution of colony-forming cells among spleen colonies. *J Cell Comp Physiol*. 1963;62(3):327-336.
4. He S, Nakada D, Morrison SJ. Mechanisms of stem cell self-renewal. *Annu Rev Cell Dev Biol*. 2009;25(1):377-406.

We found that HSCs contributed more robustly to the myeloid lineage than to the lymphoid lineage in steady state, consistent with previous reports.<sup>17,20</sup> Strikingly, platelets received the fastest and most robust influx from labeled HSCs, reaching the labeling efficiency of HSCs and complete equilibrium by 1 year after CreER activation. Moreover, the rare HPC2 population<sup>29</sup> that has been shown to possess megakaryocytic potential in vitro and upon transplantation (termed MPP2 in Pietras et al<sup>30</sup>) exhibited robust labeling from HSCs at a rate surpassing that of MPPs (also called short-term HSCs). The HPC2 population was not investigated in previous reports,<sup>16,17,20</sup> and labeling of platelets by HSCs were not traced in the studies by Sun et al and Busch et al. Recently, it was reported that the megakaryocyte lineage is the predominant fate of HSCs in the native state.<sup>33</sup> Interestingly, HSCs have been shown to produce HPC2/MPP2 after brief in vitro culture without appreciable production of MPPs (termed ST-HSCs in Pietras et al<sup>30</sup>). Therefore, it is tempting to speculate that the hierarchical order of hematopoiesis is different during native hematopoiesis than after transplantation, but further work is needed to decipher the hierarchical organization of hematopoiesis in the native state. The development of tools to lineage trace HSC progeny, such as MPPs (ST-HSC) and HPC2 (MPP2), should reveal important insights into the role of these progenitors in steady-state hematopoiesis.

## Acknowledgments

The authors thank Peggy Goodell for discussion and Catherine Gillespie for critical reading of the manuscript.

This work was supported by the National Institutes of Health (NIH), National Cancer Institute (grant R01CA193235) and National Institute of Diabetes and Digestive and Kidney Diseases (grant R01DK107413). R.H.C. was supported by the NIH, National Institute of Diabetes and Digestive and Kidney Diseases (grant T32 DK060445). Flow cytometry was partially supported by the NIH, National Center for Research Resources (grant S10RR024574), National Institute of Allergy and Infectious Diseases (grant AI036211), and National Cancer Institute (grant P30CA125123) for the BCM Cytometry and Cell Sorting Core.

## Authorship

Contribution: R.H.C., Y.-J.T., T.H., and A.K. performed the experiments and analyzed the results; M.T. performed some experiments during the early stage of the project; K.A.H. analyzed the single-cell data; and D.N. designed the research and wrote the manuscript, with input from other authors.

Conflict-of-interest disclosure: The authors declare no competing financial interests.

Correspondence: Daisuke Nakada, Department of Molecular and Human Genetics, Baylor College of Medicine, 1 Baylor Plaza, M225, Houston, TX 77030; e-mail: nakada@bcm.edu.

5. Orkin SH, Zon LI. Hematopoiesis: an evolving paradigm for stem cell biology. *Cell*. 2008;132(4):631-644.
6. Rossi L, Lin KK, Boles NC, et al. Less is more: unveiling the functional core of hematopoietic stem cells through knockout mice. *Cell Stem Cell*. 2012;11(3):302-317.
7. Kiel MJ, Yilmaz OH, Iwashita T, Yilmaz OH, Terhorst C, Morrison SJ. SLAM family receptors distinguish hematopoietic stem and progenitor cells and reveal endothelial niches for stem cells. *Cell*. 2005;121(7):1109-1121.
8. Osawa M, Hanada K, Hamada H, Nakauchi H. Long-term lymphohematopoietic reconstitution by a single CD34-low/negative hematopoietic stem cell. *Science*. 1996;273(5272):242-245.
9. Goodell MA, Brose K, Paradis G, Conner AS, Mulligan RC. Isolation and functional properties of murine hematopoietic stem cells that are replicating in vivo. *J Exp Med*. 1996;183(4):1797-1806.
10. Muller-Sieburg CE, Cho RH, Karlsson L, Huang JF, Sieburg HB. Myeloid-biased hematopoietic stem cells have extensive self-renewal capacity but generate diminished lymphoid progeny with impaired IL-7 responsiveness. *Blood*. 2004;103(11):4111-4118.
11. Dykstra B, Kent D, Bowie M, et al. Long-term propagation of distinct hematopoietic differentiation programs in vivo. *Cell Stem Cell*. 2007;1(2):218-229.
12. Sanjuan-Pla A, Macaulay IC, Jensen CT, et al. Platelet-biased stem cells reside at the apex of the haematopoietic stem-cell hierarchy. *Nature*. 2013;502(7470):232-236.
13. Yamamoto R, Morita Y, Ooehara J, et al. Clonal analysis unveils self-renewing lineage-restricted progenitors generated directly from hematopoietic stem cells. *Cell*. 2013;154(5):1112-1126.
14. Ito K, Turcotte R, Cui J, et al. Self-renewal of a purified Tie2+ hematopoietic stem cell population relies on mitochondrial clearance. *Science*. 2016;354(6316):1156-1160.
15. Sieburg HB, Cho RH, Dykstra B, Uchida N, Eaves CJ, Muller-Sieburg CE. The hematopoietic stem compartment consists of a limited number of discrete stem cell subsets. *Blood*. 2006;107(6):2311-2316.
16. Sun J, Ramos A, Chapman B, et al. Clonal dynamics of native haematopoiesis. *Nature*. 2014;514(7522):322-327.
17. Busch K, Klapproth K, Barile M, et al. Fundamental properties of unperturbed haematopoiesis from stem cells in vivo. *Nature*. 2015;518(7540):542-546.
18. Pei W, Feyerabend TB, Rössler J, et al. Polylox barcoding reveals haematopoietic stem cell fates realized in vivo. *Nature*. 2017;548(7668):456-460.
19. Schoedel KB, Morcos MNF, Zerjatke T, et al. The bulk of the hematopoietic stem cell population is dispensable for murine steady-state and stress hematopoiesis. *Blood*. 2016;128(19):2285-2296.
20. Sawai CM, Babovic S, Upadhaya S, et al. Hematopoietic stem cells are the major source of multilineage hematopoiesis in adult animals. *Immunity*. 2016;45(3):597-609.
21. Yu WVC, Yusuf RZ, Oki T, et al. Epigenetic memory underlies cell-autonomous heterogeneous behavior of hematopoietic stem cells. *Cell*. 2017;168(5):944-945.
22. Gazit R, Mandal PK, Ebina W, et al. Fgd5 identifies hematopoietic stem cells in the murine bone marrow. *J Exp Med*. 2014;211(7):1315-1331.
23. Van Keymeulen A, Mascre G, Youseff KK, et al. Epidermal progenitors give rise to Merkel cells during embryonic development and adult homeostasis. *J Cell Biol*. 2009;187(1):91-100.
24. Citri A, Pang ZP, Südhof TC, Wernig M, Malenka RC. Comprehensive qPCR profiling of gene expression in single neuronal cells. *Nat Protoc*. 2011;7(1):118-127.
25. Seita J, Sahoo D, Rossi DJ, et al. Gene Expression Commons: an open platform for absolute gene expression profiling. *PLoS One*. 2012;7(7):e40321.
26. Chambers SM, Boles NC, Lin KY, et al. Hematopoietic fingerprints: an expression database of stem cells and their progeny. *Cell Stem Cell*. 2007;1(5):578-591.
27. Chen JY, Miyanishi M, Wang SK, et al. Hoxb5 marks long-term haematopoietic stem cells and reveals a homogenous perivascular niche. *Nature*. 2016;530(7589):223-227.
28. Tajima Y, Ito K, Umino A, Wilkinson AC, Nakauchi H, Yamazaki S. Continuous cell supply from Krt7-expressing hematopoietic stem cells during native hematopoiesis revealed by targeted in vivo gene transfer method. *Sci Rep*. 2017;7:40684.
29. Oguro H, Ding L, Morrison SJ. SLAM family markers resolve functionally distinct subpopulations of hematopoietic stem cells and multipotent progenitors. *Cell Stem Cell*. 2013;13(1):102-116.
30. Pietras EM, Reynaud D, Kang YA, et al. Functionally distinct subsets of lineage-biased multipotent progenitors control blood production in normal and regenerative conditions. *Cell Stem Cell*. 2015;17(1):35-46.
31. Foudi A, Hochedlinger K, Van Buren D, et al. Analysis of histone 2B-GFP retention reveals slowly cycling hematopoietic stem cells. *Nat Biotechnol*. 2009;27(1):84-90.
32. Wilson A, Laurenti E, Oser G, et al. Hematopoietic stem cells reversibly switch from dormancy to self-renewal during homeostasis and repair. *Cell*. 2008;135(6):1118-1129.
33. Rodriguez-Fraticelli AE, Wolock SL, Weinreb CS, et al. Clonal analysis of lineage fate in native haematopoiesis. *Nature*. 2018;553(7687):212-216.